IOP Conf. Series: Materials Science and Engineering **101** (2015) 012037 doi:10.1088/1757-899X/101/1/012037

Dynamics of liquid nitrogen cooling process of solid surface at wetting contact coefficient.

P Smakulski, S Pietrowicz

Department of Thermodynamics, Theory of Machines and Thermal Systems, Wrocław University of Technology, 27 Wyb. Wyspiańskiego St., 50-370 Wrocław

E-mail: przemyslaw.smakulski@pwr.edu.pl

Abstract. Liquid cryogens cooling by direct contact is very often used as a method for decreasing the temperature of electronic devices or equipment i.e. HTS cables. Somehow, cool-down process conducted in that way could not be optimized, because of cryogen pool boiling characteristic and low value of the heat transfer coefficient. One of the possibilities to increase the efficiency of heat transfer, as well as the efficiency of cooling itself, it is to use a spray cooling method. The paper shows dynamics analysis of liquid nitrogen cooling solid surface process. The model of heat transfer for the single droplet of liquid nitrogen, which hits on a flat and smooth surface with respect to the different Weber numbers, is shown. Temperature profiles in calculation domains are presented, as well as the required cooling time. The numerical calculations are performed for different initial and boundary conditions, to study how the wetting contact coefficient is changing, and how it contributed to heat transfer between solid and liquid cryogen.

1. Introduction

Spray cooling (SC) method is one of the best ways to dissipate the heat from the surfaces with high cooling rate. Most problems of heat dissipation comes from the devices, which generate high amount of heat flux per unit area, such as microchips in hot spots, or high power laser arrays [1]. At the cryogenic temperature range, some applications, which use HTS cables also require local protection against accidental heating up to normal conducting state. It is worth mentioning that, local heat flux value within HTS cables could increase even to 10^6 W/m^2 [2].

Spray cooling by liquid nitrogen could also be applicable in tissue preservation method, using cryo-glass-freezing technique. In this area there are two basic approaches of increasing the viability of cells after its thawing. One of them contributes to high freezing rate, which would protect the delicate structure of mammal tissues before its damage [3].

Liquid nitrogen spray cooling is used not only in the field of cryopreservation technology, but also in microchips technology [4]. The fundamental limitations, which came up in the recent CPUs, are interconnect time delays and problems of dissipate the heat loads generated by computer processors. The research of D E Tilton et al. [4] provided some conception of utilizing High Temperature Superconducting (HTS) material interconnection with heat dissipation by spray cooling of liquid nitrogen. Due to positive feature of SC it is probable to maintain temperature below transition point of superconducting state for HTS cables, and also to cool down the microchips to the required level.

The paper shows the heat transfer rate determination of the liquid nitrogen spray cooling in small scale, using single droplet evaporation model in three-dimensional space system. To determine the features of solid surface cooling rate, the parameter of Wetting Contact Coefficient (WCC) is introduced.

The numerical model was performed by using two-phase Volume of Fluid method of surface tracking between phases. All the simulations were carried out with the usage of the OpenFOAM 2.3.0 toolkit environment.

2. Small scale analysis

Hydrodynamic and thermal influence of impacted droplets onto flat surface are coupled and dependent from each other. Droplets created in the sprays reach the surface and have an effect with heated surface in a short period of time, with is a highly complicated process, depends on a kinetic energy of the droplet during impingement [5]. A process of shape formation mostly depends on viscosity, inertia and surface tension forces [6]. Interface contact formation starts with liquid spreading and wetting of solid surface, which was proved in [2,3] that mentioned process is much faster than heat transfer between two mediums. To compare different behavior of droplets, the dimensionless Weber number was implemented, as the ration between inertia forces to surface tension forces of the droplet.

$$We = \frac{\rho_l d_0 v_0^2}{\sigma}, \quad (1)$$

where: ρ_l – liquid density; d_0 – initial droplet diameter; v_0 – initial droplet velocity; σ - liquid surface tension. It is shown in the publications [1, 2, 9] that, when liquid achieves the critical Weber number, droplets could divide into smaller particles. The critical value of *We* depends on liquid type and is experimentally determined, but in most cases it is assumed to be around 14 [10].

Heat transfer of single droplet is determined by initial temperature of the drops, walls, and environment, as well as partial pressures between liquid-vapor interface and partial pressure in some distance from interface [6]. As it was shown in [11] heat transfer process of single droplet occurs at time-varying wetting surface.

Heat transfer for sprays in macro-scale mostly depends on sparging density. Together with the increase of liquid sparging density, the heat transfer rate from the flat surface grows. Sparging density is described as a ratio of volumetric flow rate to active surface area perpendicular to the direction of the liquid flow [10]. In small-scale (for a single droplet), analogous coefficient of wetting contact surface (WCC) could be introduced according to the study of [6]. This coefficient defines area occupied by spread liquid to initial diameter of the droplet treated as an ideal sphere:

$$\beta = \frac{D_r}{d_0}, \quad (2)$$

D_r – imaginary diameter of the wetting circle, on which droplet interacts; d_0 – initial droplet diameter.

3. Numerical method

The numerical calculations were carried out with the usage of OpenFoam software where the set of discretized Navier Stokes (NS) linear equations were solved. OpenFOAM libraries implement a finite volume elements method (FVM) of second order of convergence with support of arbitrary unstructured meshes.

3.1. Numerical model of phase change.

Subject to heat transfer rate during dynamics of liquid nitrogen droplet propagation on a flat and perfectly smooth surface, was under consideration in this study. To analyze the impact of WCC on the heat flux, a liquid nitrogen droplet having a diameter of 1.0 mm was selected, to allow better observation of the influence of liquid spread on thermal problems.

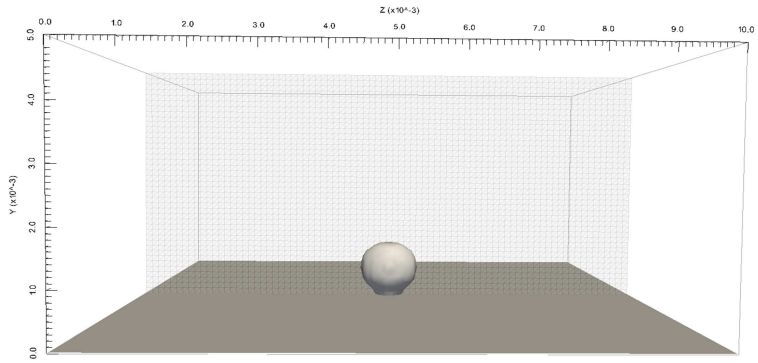

Figure 1. Numerical domain.

Contact surface boundary condition between solid and liquid, was implemented as 1.0 mm thick material surface. Additional material was introduced as a virtual domain of solid, on which temperature profile was calculated assuming a one-dimensional heat transfer process from the bottom of a virtual domain, with steady temperature value as a boundary condition. All calculations for the one-dimensional heat transport problem were performed by the equation shown in (3). This pseudo-conjugate heat transfer helps to developed the temperature profile on a hot surface, during simulation time.

$$\rho_m c_{p_m} \frac{\partial T}{\partial \tau} = k_m \frac{\partial^2 \mathrm{T}}{\partial x^2} - \dot{q}, \tag{3}$$

where: c_p is heat capacity, ρ – density, k is thermal conductivity, m subscript represent the properties of material declared, $\dot{q}$ is a heat flux forced by evaporation. Approximation of 1D heat transfer in virtual solid was justified by calculated issues on a small scale. Temperature of the contact surface was being updated during each time step after passing the main program loop.

The simulation has been considered for the three types of solids, used in cryogenics: aluminum, stainless steel SS 304, and Kapton. As an initial temperature for the contact surface was established at the value of 83 K, which corresponds to working temperature of HTS cable Bi-2223 producing around 0.1 T of magnetic field [13]. Initial temperature for the liquid nitrogen droplet was fixed to temperature of phase change under atmospheric pressure (77 K). Maximal temperature differences between solid and liquid ensures that during simulations, evaporation process occurs in nucleate boiling regime.

To develop single liquid particle behavior, a numerical method of interface surface tracking called Volume of Fluid (VoF) was used [14]. Phase border is calculated by introducing additional liquid fraction function. This function gives a parameter value declared as a volume ration of liquid in individual numerical mesh cell to overall cell volume. Introducing the new parameter allows computing a set of NS equations by Euler method, treats a values of density, kinematic viscosity, and other two-phase parameters, the same as in one-phase system, thanks to the average representation of two phases' properties (see equations 6,7,8). However, when the two-phase system with the transition phase is considered, this approach may enter additional disorders, treating the equation of energy throughout the mesh volume uniformly. This may lead to a situation in which evaporation (under appropriate thermodynamic conditions) will occur in the whole volume of liquid uniformly, rather than on the interface itself. In order to eliminate unfavorable effects related to the calculation taken by VOF method, the authors have placed additional solver algorithm for detecting the gradient of the interface by introducing *Heaviside* functions, to obtain sharp edge of phase transition. Similar treatment of the problem could be found in [15]. Heaviside function is used for reconstructing the

interface between liquid and vapor of the nitrogen. This approach takes place in order to estimate better the mutual properties of each mesh cells around a well situated interface surface.

Energy equation of phase transition is shown below (4). Presented source term of heat flux forced by evaporation ($\dot{q}$) is coupled with heat flux source term in equation (3).

$$\frac{\partial T}{\partial \tau} + \nabla \cdot (\boldsymbol{U}T) = DT\ \nabla^2 \mathrm{T} - \frac{\dot{q}}{\rho\ c_p} \tag{4}$$

$$\dot{q} = \begin{cases} -\dot{m}_{lv}\ L & for\ evaporation \\ \dot{m}_{lv}\ L & for\ condensation \end{cases} \tag{5}$$

DT – diffusion coefficient, ***U*** is velocity vector, $\dot{m}_{lv}$ denotes for mass stream of evaporated medium condensate, and *L* is for a latent heat of evaporation. It was assumed that the most important in the heat transfer was the mechanism of diffusion and convection. The impact of radiation has been skipped, due to the fact of relatively small difference in temperature between solid and liquid. Two-phase properties such as specific heat, density, and viscosity were defined as weighted average parameters, wherein the weight ratio of the parameter corresponds to the function of liquid fraction in two-phase system. The fluid flow within the domain was treated as incompressible.

$$\rho = \alpha\ \rho_{liq} + (1-\alpha)\rho_{gas} \tag{6}$$

$$\mu = \alpha\ \mu_{liq} + (1-\alpha)\mu_{gas} \tag{7}$$

$$c_p = \alpha\ c_{p_{liq}} + (1-\alpha)c_{p_{gas}} \tag{8}$$

Weighted average properties in two-phase system (liquid-gas), where
μ – viscosity, α – phase fraction parameter were presented above.

Detailed information regarding initial and boundary conditions are described in the table 1. All the series of calculation were performed for three different types of solid surface materials.

Table 1. Boundary and initial conditions for simulation.

Case	Wall temperature	Initial droplet temperature	d_0	Initial droplet velocity	*We*
1	83 K	77 K	1.0 mm	0.1 m/s	1.0
2	83 K	77 K	1.0 mm	0.5 m/s	21.5
3	83 K	77 K	1.0 mm	1.0 m/s	85.9

A hexagonal numerical grid of dimension of 10x5x10 cm, divided into 80, 40 and 80 finite elements in each dimension respectively, was used. All numerical calculations were carried out by means of direct numerical simulation (DNS) technique.

4. Model validation

Mathematical model described above has been benchmarked in terms of fluid dynamic propagation at the given flow conditions, as well as for the transport of heat transfer through evaporation forced by nucleate boiling. Due to limited availability of information on dynamics propagation of a single liquid nitrogen droplet on a solid surface in literature, it was decided to compare the model with the experimental results available in the literature, concerning the well-known spreading dynamics of water drop [5]. On the other hand, evaporation of liquid nitrogen was compared with experimental results contained in the publications [15, 16] and performed for pool boiling. In this part, the achievable heat flux values in relation to the temperature difference between solid surface and liquid nitrogen, was treated as a comparative values.

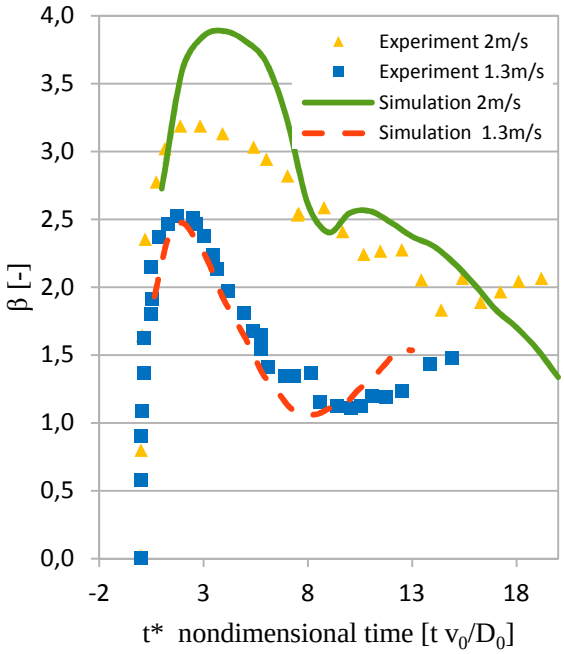

Figure 2. Hydrodynamic propagation of impinged droplet of water – in comparison with [5].

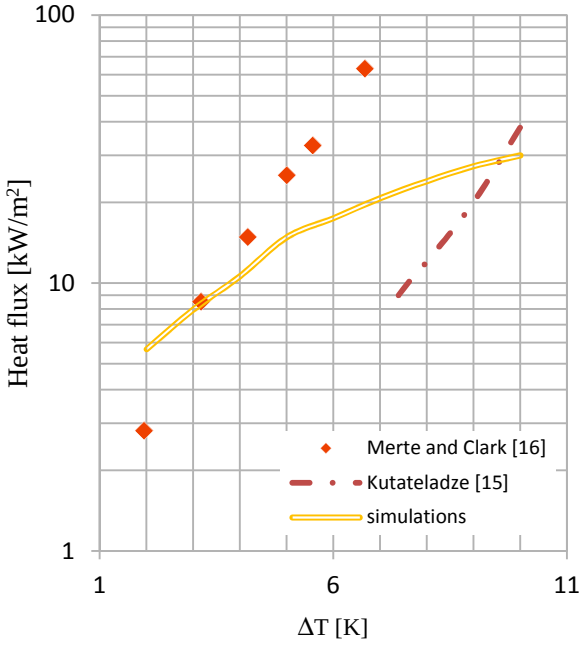

Figure 3. Pool boiling heat flux in comparison with literature data published in [15, 16].

As it can be seen, the results of fluid dynamics propagation on a solid flat surface gave a satisfactory compatibility to the experimental results (figure 2). On the other hand, the curve obtained from the simulations for pool boiling (figure 3), is in the range of experiments contained in the [15, 16]. However, the angle of inclination of the curve obtained from numerical simulation does not fully covers experimental profiles. This may be due to disregarding the compressibility features of fluid in the above-mentioned numerical model.

5. Results

The results of numerical simulations for droplet propagation in small scale have been illustrated below. The process of heat transfer at the time of liquid droplet formation after impact with a solid surface has been considered. In all simulations the time constants up to values of 30 ms were considered. After this time rate the formation of a droplet shape (or secondary droplets), was finished. It is noted that the distribution of liquid achieved small *We* numbers (of approx. 1.0) during the formation of the final shape, do not defragment into smaller particles at all. Its surface has been established to the final form of a hemisphere. In contrast to that, a droplet with the *We* values 21.5 and 85.9 followed by a re-fragmentation (secondary breakup) of the liquid, which also affected the WCC and has an impact on the reached heat flux.

Figures 4-11 show a field temperature during a droplet impact. All figures presented below are shown for aluminum, specified as the cooled material.

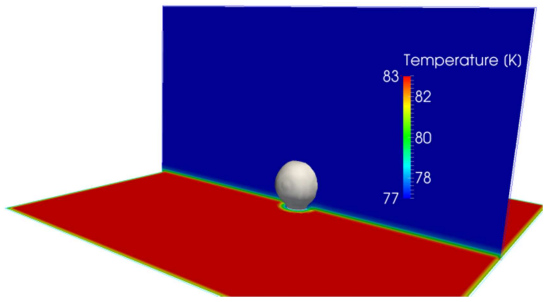

Figure 4. Temperature profile of the heated surface during impact. *We* = 1.0, time = 1ms.

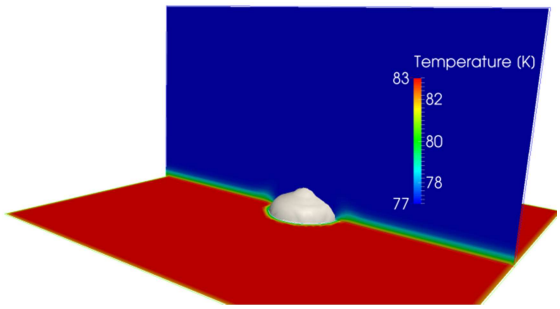

Figure 5. Temperature profile of the heated surface during impact. *We* = 1.0, time = 5ms.

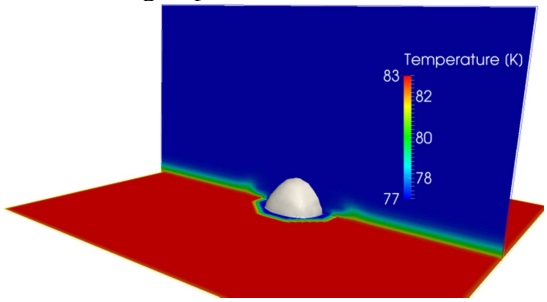

Figure 6. Temperature profile of the heated surface during impact. *We* = 1.0, time = 10ms.

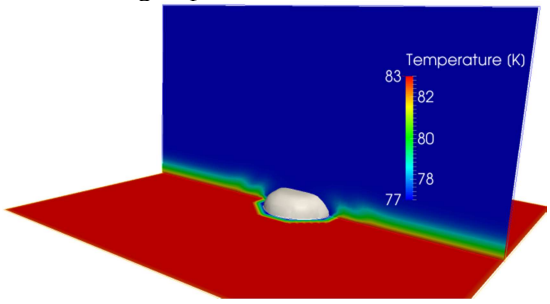

Figure 7. Temperature profile of the heated surface during impact. *We* = 1.0, time = 20ms.

As it can be seen in Figures 8-11 with higher Weber numbers, heat transfer from the solid surface occurs at a much larger area in relation to the fluid dynamics at lower Weber numbers (figures 4-7).

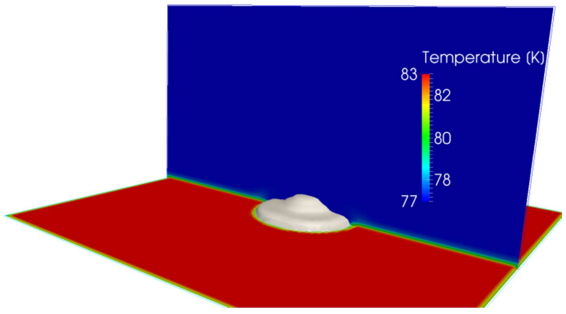

Figure 8. Temperature profile of the heated surface during impact. *We* = 85.9, time = 1ms.

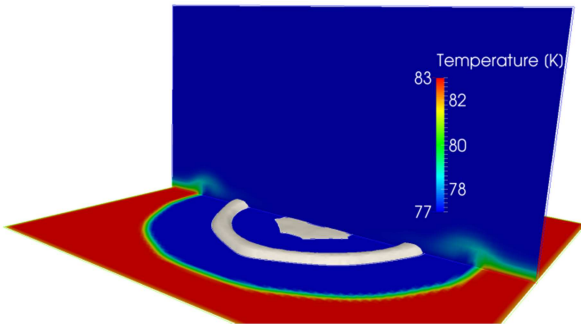

Figure 9. Temperature profile of the heated surface during impact. *We* = 85.9, time = 5ms.

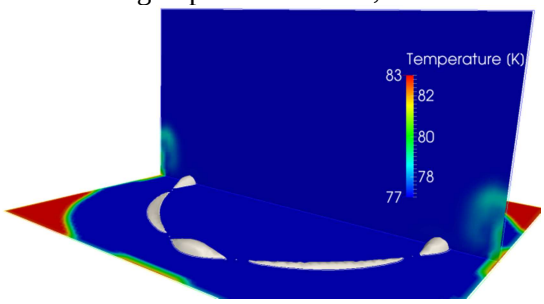

Figure 10. Temperature profile of the heated surface during impact. *We* = 85.9, time = 10ms.

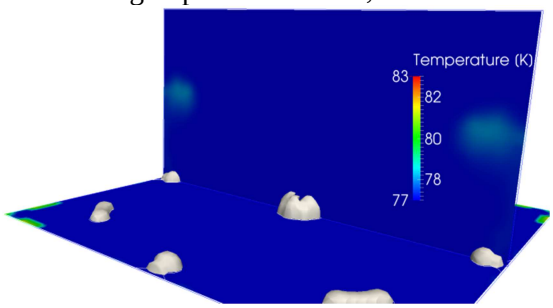

Figure 11. Temperature profile of the heated surface during impact. *We* = 85.9, time = 20ms.

The values of the heat flux obtained from the solid surface varies, depending on the initial liquid drop performance parameters. Numerical simulations show that the importance of liquid distribution and its coefficient of WCC on heat transfer process. The larger the surface area of liquid in contact with the solid body, the higher heat flux parameters could be achieved.

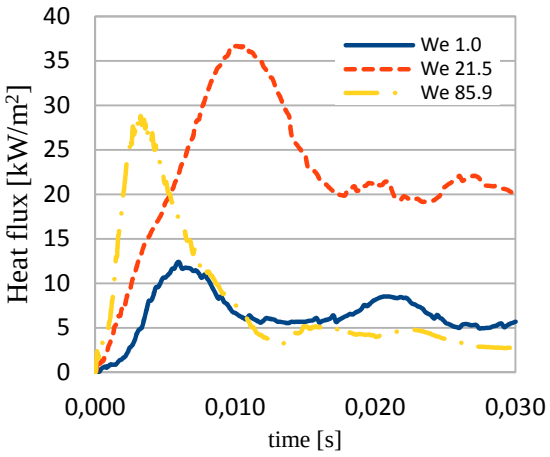

Figure 12. Heat flux during the impact time for different *We* numbers.

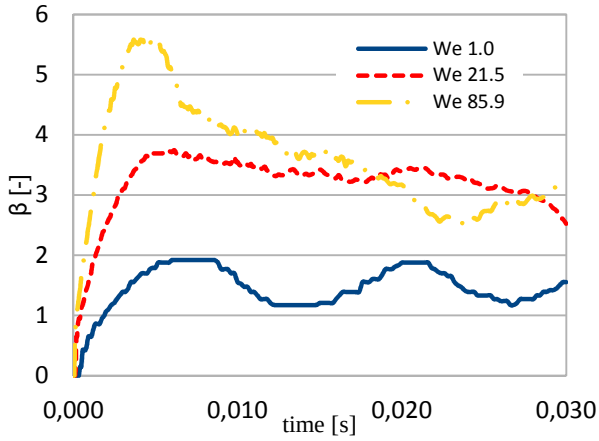

Figure 13. Wetting contact coefficient during the impact time for different *We* numbers.

It was also observed in figure 12 that the heat flux reaches its maximum value at a certain time after impact with the surface. Their peak values correspond to the maximal wetting contact coefficient, and depend on applied solid surface material (figure 14). It is also worth mentioning, that the highest peak of the heat flux correlate with the middle value of *We* in this research, not for the highest one.

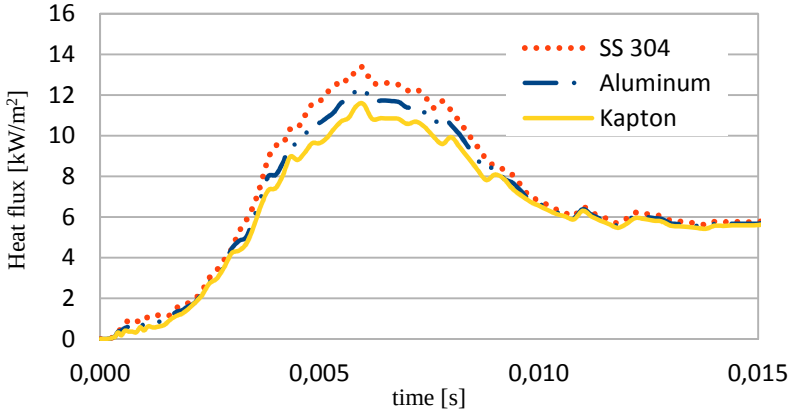

Figure 14. Peak heat flux for different materials declared as a boundary condition.

6. Summary

The three-dimensional model of droplet evaporation was presented and benchmarked by the results of the experiment included in literature. The simulation results illustrate the behaviour of a single particle of liquid nitrogen during impact on a heated solid surface. Dynamics of liquid spilling significantly affect the removal of heat transfer from the surface. Heat flux rate changes proportionally to wetting contact coefficient.

As it can be seen above, the cooling of the surface occurs immediately after the particle collision on the flat surface. Time constants of 30 milliseconds show that upon an impact, the highest heat flux

values are characterized by the instances at which the Weber number reaches values of 21.5 or 85.9. With both of those Weber numbers, fragmentation of a single droplet, which significantly enlarge the field of the influence, has been occurred (β above 2 – see figure 13).

Acknowledgment
Calculations have been carried out by the usage of the resources provided by Wroclaw Centre for Networking and Supercomputing (http://wcss.pl), grant No. 279 and 309.

References

[1] Smakulski P 2013 *Method of high heat flux removal by usage of liquid spray cooling* Arch. Thermodyn. 34 173–84
[2] Maninder S S, Luis C C, Ottfried J H and Martin R P 1995 *Spray cooling of power electronics at cryogenic temperatures* J. Thermophys. Heat Transf. 9 123–8
[3] Zhmakin A I 2009 *Fundamentals of Cryobiology* ed A I Zhmakin (Berlin, Heidelberg: Springer Berlin Heidelberg)
[4] Tilton D E, Kearns D A and Tilton C L 1994 *Liquid nitrogen spray cooling of a simulated electronic chip Adv. Cryog. Eng.* 39 1779–86
[5] Manzello S L and Yang J C 2002 *An experimental study of high Weber number impact of methoxy-nonafluorobutane C4F9OCH3 (HFE-7100) and n -heptane droplets on a heated solid surface* Int. J. Heat Mass Transf. 45 3961–71
[6] Zapalowicz Z 2007 *Oddziaływanie strumienia kropel i powietrza na powierzchnię ciała stałego* (Szczecin: WUPS) (in Polish)
[7] Trapaga G and Szekely J 1991 *Mathematical Modeling of the Isothermal Impingement of Liquid Droplets in Spraying Processes* Metallurgical Transactions B 22 901-914
[8] Ishimoto J, Oh U, Guanghan Z, Koike T and Ochiai N 2014 *Ultra-high heat flux cooling characteristics of cryogenic micro-solid nitrogen particles and its application to semiconductor wafer cleaning technology* Advances in cryogenic engineering 1573 1099–106
[9] Zapalowicz Z 1995 *Analysis of the process of wetting a horizontal heated surface area by a single water droplet* Int. Commun. heat mass Transf. 22 713–20
[10] Orzechowski Z and Prywer J 2008 *Wytwarzanie i zastosowanie rozpylonej cieczy* (Warszawa: WNT) (in Polish)
[11] Strotos G and Gavaises M 2008 *Numerical investigation on the evaporation of droplets depositing on heated surfaces at low Weber numbers* Heat Mass Transf. 51 1516–29
[12] Marić T, Hopken J and Mooney K 2014 *The OpenFOAM Technology Primer* (sourceflux UG)
[13] Eltsev Y, Lee S, Nakao K and Tajima S 2010 *The electrical transport properties of high quality Bi-2223 crystal* Sci. Technol. 10–3
[14] Hirt C and Nichols B 1981 *Volume of fluid (VOF) method for the dynamics of free boundaries* J. Comput. Phys. 39 201–25
[15] Kida M, Kikuchci Y, Takahashi O and Michiyoshi I 1981 *Pool-Boiling Heat Transfer in Liquid Nitrogen* J. Nucl. Sci. Technol. 18 501–13
[16] Merte H and Clark J A 1962 *Boiling heat-transfer data for liquid nitrogen at standard and near-zero gravity* Advances in cryogenic engineering 7 546–50